

To be published in *Electronic Surface and Interface States on Metallic Systems*, eds.: E. Bertel und M. Donath (World Scientific, Singapore, 1995).

## Frustrated H-induced Instability of Mo(110)

P. Ruggerone, B. Kohler, S. Wilke, and M. Scheffler

*Fritz-Haber-Institut der Max-Planck-Gesellschaft, Faradayweg 4-6, D-14195 Berlin-Dahlem, Germany*

### ABSTRACT

The large interest in the properties of transition metal surfaces has been recently fostered by inelastic helium atom scattering experiments carried out by Hulpke and Lüdecke. Sharp and giant anomalies in the surface phonon dispersion curves along  $\overline{\Gamma\text{H}}$  and  $\overline{\Gamma\text{S}}$  have been detected on W(110) and Mo(110) at a coverage of one monolayer of hydrogen. At the same critical wave vectors a smaller second indentation is present in the experimental phonon branches. Recently we have proposed a possible interpretation which is able to explain this and other experiments. In this paper we discuss results of our recent ab initio calculations of the atomic and electronic properties of the clean and H-covered Mo(110) surface in more details. For the full monolayer coverage the calculated Fermi-surface contours are characterized by strong nesting features which originate the observed anomalies.

### 1. Introduction

The original goal of the inelastic helium atom scattering (HAS) investigation on H/W(110) performed by Hulpke and Lüdecke<sup>1-3</sup> was to find a lattice dynamical fingerprint of the so called *top-layer-shift reconstruction*.<sup>4</sup> This structural model was proposed by Estrup and coworkers<sup>4</sup> to explain their low energy electron diffraction (LEED) data with hydrogen adsorbed on the surface: the presence of hydrogen induces a rigid shift along the  $[\overline{1}10]$  direction of the top layer atoms with respect to the substrate. However, the size of this suggested displacement is still under discussion and no evidence for such a rearrangement has been reported for H/Mo(110).<sup>5</sup> The HAS data did not offer insight into the mechanism of the top-layer-shift reconstruction, but were quite amazing. On W(110) and Mo(110) the HAS data for the clean phase

do not exhibit any peculiarities, whereas for a full monolayer of hydrogen the surface phonon dispersion curves are characterized by two anomalous indentations which both occur at the same critical wave vector  $\mathbf{Q}_{c1}^{\text{exp}}$  along the [001] direction ( $\overline{\Gamma\text{H}}$ ).  $\mathbf{Q}_{c1}^{\text{exp}}$  has a length of  $0.95 \text{ \AA}^{-1}$  for W and  $0.90 \text{ \AA}^{-1}$  for Mo. The dips have been also detected along directions deviating from  $\overline{\Gamma\text{H}}$ . In particular, along the  $[\overline{112}]$  direction ( $\overline{\Gamma\text{S}}$ ) the indentations occur at the  $\overline{\text{S}}$  point for Mo and very close to it for W, having the critical wave vector  $\mathbf{Q}_{c2}^{\text{exp}}$  length of  $1.225$  and  $1.218 \text{ \AA}^{-1}$  for W and Mo respectively. Since the experimental curves are available only for  $\overline{\Gamma\text{H}}$  and  $\overline{\Gamma\text{S}}$  (see Ref. 3), we focus our attention on these two cases characterized by strong and well defined anomalies in the phonon branches. For both systems two different dips in the surface dispersion curves were observed at the critical wave vectors: a smaller softening and a very sharp and localized indentation from  $\hbar\omega \approx 15 \text{ meV}$  to  $\hbar\omega \approx 2 \text{ meV}$ . Similarly deep and sharp anomalies in the phonon branches have been detected only in neutron scattering experiments on quasi-one-dimensional conductors, like KCP  $[\text{K}_2\text{Pt}(\text{CN})_4\text{Br}_3]$ ,<sup>6</sup> but never on surfaces. A pronounced but less sharp damping of longitudinal surface phonons was detected on the (100) surfaces of W<sup>7,8</sup> and Mo<sup>9</sup> and was interpreted as a soft phonon due to a Kohn anomaly involving electronic surface states at the Fermi level.<sup>10,11</sup> In the case of W(100) the Fermi surface nesting is particularly efficient and drives a structural rearrangement of the atomic pattern leading to a  $c(2 \times 2)$  reconstruction at temperatures below  $T_c \approx 250 \text{ K}$  (for a review see Ref. 12). As already mentioned, the phonon dispersion curves for the clean (110) surfaces do not present any unusual features; the anomalies appear only when one monolayer of hydrogen is adsorbed. However, it seems that hydrogen vibrations do not play a crucial role in the appearance of the indentations, because the HAS spectra do not change when deuterium is adsorbed instead of hydrogen.<sup>2,3</sup> Moreover, a possible link between the anomalies and the top-layer-shift reconstruction should be ruled out because the dips were also observed on H/Mo(110) which does not exhibit any experimental evidence of a pronounced atomic rearrangement. As in the case of the (100) surface of the same systems the interpretation of such a vibrational behaviour in terms of Fermi surface effects should be supported by the presence of electronic surface states connected by nesting wave vectors comparable with the critical ones resulting from the HAS spectra. However, angular resolved photoemission (ARP) studies carried out by Kevan and coworkers<sup>13-15</sup> do not show any evidence of parallel segments of the Fermi-surface contours and thus a nesting origin of the HAS anomalies was ruled out in these analyses.

The jigsaw puzzle was even more complicated by the data from a very

careful high resolution electron energy loss spectroscopy (HREELS) investigation on hydrogen covered W(110)<sup>16,17</sup>: The experimental points pin down the dispersion of the small anomaly (in perfect agreement with the HAS data), but not of the huge indentation. Thus, the latter is only visible in helium scattering. Moreover, the HREELS spectra for the high energy adsorbate vibrations, which are not accessible to the HAS experiment, are also characterized by an anomalous behaviour. At a coverage of 1 ML of hydrogen the peaks due to the adsorbate vibrations parallel to the surface are no more resolved in the HREELS spectra as *single* inelastic structures but give rise to a broad continuum. These features were explained by Balden *et al.*<sup>17</sup> as being due to the fact that at that coverage the hydrogen atoms form a quantum fluid. Within the framework of this picture the sharp anomaly is an elementary excitation of this fluid similar to a roton.<sup>18</sup> We like to stress, however, that this interpretation of the huge indentation fails because it involves vibrations of the hydrogen, and therefore predicts strong isotopic effects, which have not been observed in the HAS experiments.<sup>1-3</sup> Moreover, to the best of our knowledge the typical dispersion of a roton is not as sharp as the one seen in the case of H/W(110) and H/Mo(110). While we question the "roton idea", we feel that the experimental evidence for a liquid phase is indeed strong and calls for a detailed analysis.

In this paper we review the results of a recent *ab-initio* study<sup>19</sup> which provide new insight into these unusual and exciting phenomena. Our results for the atomic and electronic structure of the clean and H-covered Mo(110) surfaces are presented and discussed in view of the two anomalies and of the ARP data. Finally, in the Conclusion we comment on some still open question.

## 2. Results

We employed the density-functional theory (DFT) together with the local-density approximation for the exchange-correlation energy functional,<sup>20</sup> using the full-potential linearized augmented plane wave (FLAPW) method<sup>21</sup> for the self-consistent evaluation of the Kohn-Sham equation, total energy, and forces.<sup>22,23</sup>

The surfaces are modeled by a seven layer slab for the Mo(110) substrate repeated periodically with a separation of 8.8 Å vacuum. A mesh of 64 equally spaced points in the surface Brillouin zone (SBZ) is employed for the integration in the reciprocal space. The muffin-tin radii are chosen to be 1.27 Å and 0.48 Å for Mo and H, respectively. The kinetic-energy cutoff for the plane wave

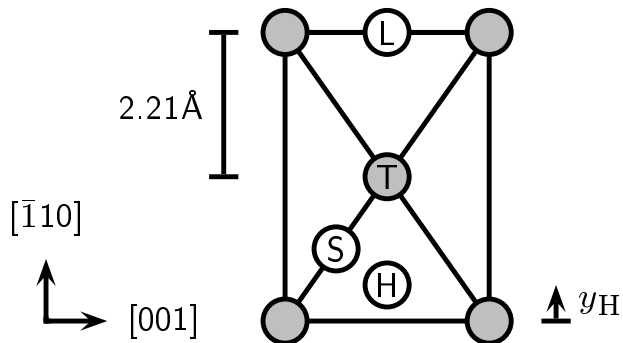


Fig. 1. Surface geometry of Mo(110) with the long-bridge (L), short-bridge (S), hollow (H) and on-top (T) sites marked.  $y_H$  is the  $[110]$ -offset of the hollow position from the long-bridge site.

basis needed for the interstitial region is set to 12 Ry, and the  $(l, m)$  representation (inside the muffin tins) is taken up to  $l_{\max} = 8$ . For the potential expansion we use a plane-wave cutoff energy of 64 Ry and a  $(l, m)$  representation with  $l_{\max} = 4$ . The core states as well as the valence states are treated non-relativistically. The calculated in-plane lattice constant is 3.13 Å without including zero point vibrations, which compares well with the measured bulk lattice parameter (3.148 Å at room temperature<sup>24</sup>). The values of the surface relaxation for the clean surface (see Table 1, first column) are in excellent agreement with those calculated by Methfessel *et al.*<sup>25</sup> who employed the full-potential linearized muffin-tin orbitals approach.<sup>26</sup>

Our first goal is the determination of the geometry of the system, of the relaxation parameters, and of the energetics of the possible hydrogen adsorption sites for the full monolayer coverage. For this coverage there is one hydrogen atom per unit cell and the four possibly important adsorption positions are depicted in Fig. 1. They are the long-bridge (L), short-bridge (S), hollow (H) and on-top (T) sites. The results of the calculations are collected in Table 1. Clearly, the hollow site appears as the energetically most favorable site, while the difference in energies between the long-bridge and short-bridge positions is small. On the other hand, a hydrogen in the on-top location ap-

	clean	hollow	long bridge	short bridge	on top
$d_{\text{H-Mo}}$ (Å)	—	1.07	1.08	1.32	1.76
$\Delta d_{12}$ ( $\%d_0$ )	-4.5	-2.1	-1.9	-2.8	+1.8
$\Delta d_{23}$ ( $\%d_0$ )	+0.5	+0.1	-0.1	+0.3	-1.2
$\Delta d_{34}$ ( $\%d_0$ )	0.0	-0.1	-0.3	-0.3	+0.1
$\Delta E_{\text{ad}}$ (eV)	—	0.0	-0.23	-0.28	-1.11

Table 1. Calculated geometries and adsorption-energy differences for clean Mo (110) and for the H-covered surface. For the latter the results for the long-bridge, short-bridge, hollow, and on-top sites (see Fig. 1) are compiled. The height of the hydrogen atom above the surface is denoted as  $d_{\text{H-Mo}}$  and  $\Delta d_{ij}$  is the percentage change of the inter-layer distance between the  $i$ -th and the  $j$ -th layer with respect to the bulk inter-layer spacing  $d_0$ .

pears definitely unstable. To find the exact position of the adsorbate we start with the hydrogen in the long-bridge position and we allow its relaxation according to the forces. The hydrogen relaxes directly into the hollow site finding its stable geometry at a position  $y_{\text{H}} = 0.55 \pm 0.01 \text{ \AA}$  (see Fig. 1). We do not find a pronounced top-layer-shift reconstruction which is in agreement with an analysis of low-energy electron diffraction experiments.<sup>5</sup> A comparison with the calculated clean surface geometry shows that adsorption of hydrogen produces a reduction of the inward relaxation as expected. In the case of the on-top adsorption site the relaxation becomes even outwards. Note that the numerical error for all calculated inter-layer spacings is about  $\pm 0.3 \%d_0$ . Table 1 shows that the differences in energy among the adsorption sites are similar to those found for other systems, H/Pd(100) and H/Rh(100).<sup>27,28</sup> We should point out that the investigation of Balden *et al.* was carried out on H/W(110) and HREELS experiments on H/Mo(110) are in progress. However, our preliminary results on H/W(110) show similar adsorption energies for the four sites. Therefore, our results do not seem to rule out the presence of a liquid-like phase of the hydrogen atoms on W(110).

After having determined the energetically most stable geometry we calculated the electronic properties of the surface in both phases, clean and covered with a full monolayer of hydrogen. The theoretical results for the Fermi-surface contours are collected in Fig. 2 (left panels) together with experimental ARP data of Jeong *et al.*<sup>14</sup> (Fig. 2, right panels). The solid (dotted) lines label surface resonances or surface states which are localized by more than 60 % (30 %) in the two top Mo layers. For the adsorbate system we present the results

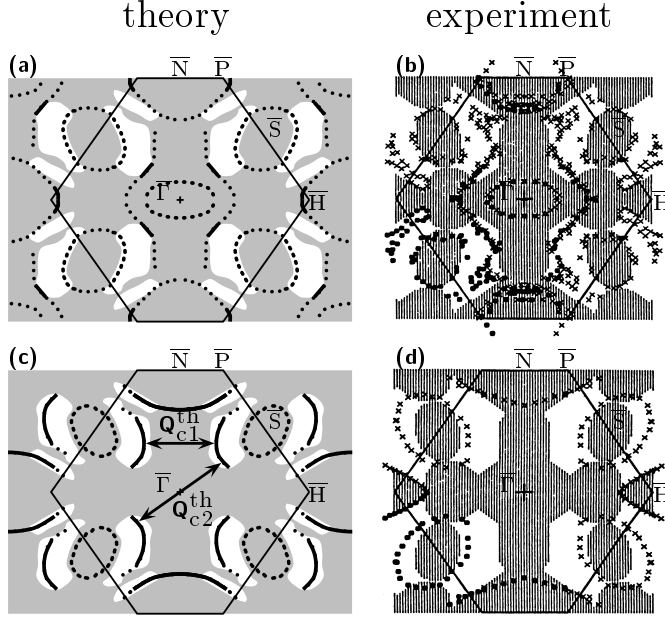


Fig. 2. Fermi surfaces of clean Mo(110) [upper panels] and Mo(110) with a full monolayer of hydrogen [lower panels]. The experimental results are from Ref. 14. Shaded areas are the projection of the bulk Fermi surfaces onto the (110) surface Brillouin zone. The solid (dotted) lines of the theoretical results denote surface resonances or surface states which are localized by more than 60 % (30 %) in the two top Mo layers.  $\mathbf{Q}_{c1}^{th}$  and  $\mathbf{Q}_{c2}^{th}$  are the critical wave vectors, predicted by the calculations.

for the hollow position.

The shaded area is the projection of the bulk Fermi surface onto the SBZ of the (110) surface. For the experimental analysis Jeong *et al.* calculated this projection using a semiempirical tight-binding interpolation scheme.<sup>29</sup> The differences between the results (left and right panels in Fig. 2) for the projected bulk Fermi surface (shaded areas) may arise from the lack of self-consistency of the tight-binding approach. We notice that in Fig. 8 of Ref. 14 Jong *et al.* presented results with their Fermi level shifted up by 200 meV. In this case a good agreement of their results with our DFT-LDA is achieved. For the clean surface (see Fig. 2a) our calculations identify four bands, which are highly localized at the surface. They give rise to Fermi-surface contours of which one is centered at  $\bar{\Gamma}$ , one at  $\bar{S}$ , one at  $\bar{N}$ , and one which runs more or less parallel to the  $\bar{\Gamma}\bar{N}$  direction. The latter has  $(d_{3z^2-r^2}, d_{xz})$  character, and also the other surface features originate from Mo *d* bands. All of these bands have been detected experimentally, and for all of them the calculated and measured

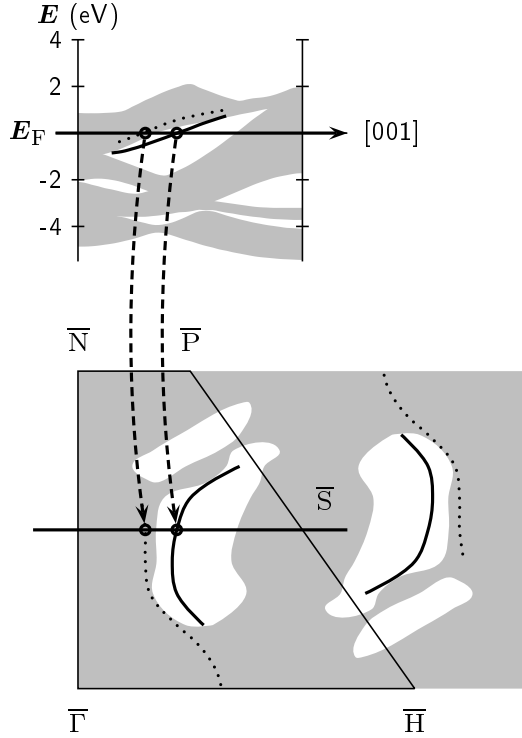


Fig. 3. Band structure (upper figure) and Fermi surface (lower figure) of clean Mo(110) (dotted curves) and H/Mo(110) (solid curves). The shaded areas are the projection of the Fermi surface onto the SBZ of the bcc (110) surface.

$\mathbf{k}$ -dependence is in very good agreement (compare Figs. 2a and b). On the other hand, the comparison for the adsorbate systems (see Figs. 2c and d) shows a clearly worse agreement.

At first we discuss the changes of the theoretical Fermi surface induced by the hydrogen adsorption (Fig. 2a and c), and then we return to the experimental results. For the present discussion the most important effect is that the  $(d_{3z^2-r^2}, d_{xz})$  band is shifted away from the  $\overline{\Gamma\bar{N}}$  line. This effect can be better viewed in Fig. 3. On the clean surface the  $(d_{3z^2-r^2}, d_{xz})$  (dotted line) state is present, but it is buried in the bulk band density of states. After adsorption of a full monolayer of hydrogen, a significant fraction of the band has been shifted into the stomach shaped band gap. This shift reflects the change in the surface potential due to the screening of the hydrogen adatom induced perturbation by the easily polarizable surface  $d$  electrons. In the *frontier orbital* picture proposed by Hoffmann<sup>30</sup> the hydrogen  $s$ -orbital interacts mainly with occupied states close to the bottom of the  $d$ -band. Whereas the corresponding bonding states are situated 5 eV below the Fermi level, the antibonding states,

which would be partly occupied, are at higher energies (about 4 eV above the Fermi energy) and they will dump their electrons at the Fermi level. As a consequence, the corresponding occupation redistribution to states at  $E_F$  gives rise to the observed decrease of the surface potential a shift of the entire  $(d_{3z^2-r^2}, d_{xz})$  band to lower energies occurs. As this band disperses upward when  $\mathbf{k}$  increases away from  $\bar{\Gamma}$ , the Fermi energy cuts the shifted band at wave vector with a larger component along  $\bar{\Gamma\bar{H}}$ . In addition, we notice the important fact that no strong changes in the form of the Fermi-surface orbits are observed in our results when we (artificially) place the hydrogen atom in the short-bridge or long-bridge positions.

Figures 2c and 3 reveal that the Fermi-surface contours associated to the  $(d_{3z^2-r^2}, d_{xz})$ -like band run parallel to the  $\bar{\Gamma\bar{N}}$  direction and perpendicular to  $\bar{\Gamma\bar{S}}$  in significant parts of the SBZ giving rise to a quasi-one-dimensional nesting. The  $\mathbf{k}$ -vectors connecting these bands in different sections of the Brillouin zone are labeled in Fig. 2c with  $\mathbf{Q}_{c1}^{\text{th}}$  and  $\mathbf{Q}_{c2}^{\text{th}}$ . We recall that in DFT the highest occupied Kohn-Sham level of the self-consistent  $N$ -electron calculation corresponds to the electron chemical potential, i.e., the Fermi *level*. However, the Kohn-Sham Fermi *surface* is (in principle) not an observable. On the other hand, the agreement between Fig. 2a and b and the fact that the wave function character does not change significantly upon hydrogen adsorption support the hypothesis that the difference between the Kohn-Sham Fermi surface and the true Born-Oppenheimer Fermi surface is not very important for this system. We therefore conclude that the nesting instability predicted by the Fermi surface of Fig. 2c can be trusted. Moreover, the dispersion of the  $(d_{3z^2-r^2}, d_{xz})$  band in Fig. 3 is flat and the associated electronic density of states at the Fermi level is high. Therefore, a large number of electrons are involved in the nesting and the mechanism increases its efficiency. Because of this aspect and due to its nearly one-dimensional nature we expect important consequences.<sup>31</sup> Such an instability may produce a static rearrangement of the atoms provided that the electronic energy gain is stronger than the elastic energy cost needed to distort the atomic lattice. This is the case of the (100) surface of Mo and W, where this kind of distortion accompanied by the appearance of a charge density wave occurs below a critical temperature. Because the (110) surface is the closest packed and most stable bcc surface such a Peierls distortion is hampered and somewhat unlikely. When the system does not undergo a static distortion, strong dynamical consequences (similar to a dynamical Jahn-Teller effect in molecules) will take place due to thermally excited electron-hole pairs with a wave vector equal to the critical wave vectors and their coupling to surface phonons. In other words, the electronic system is close to an instability

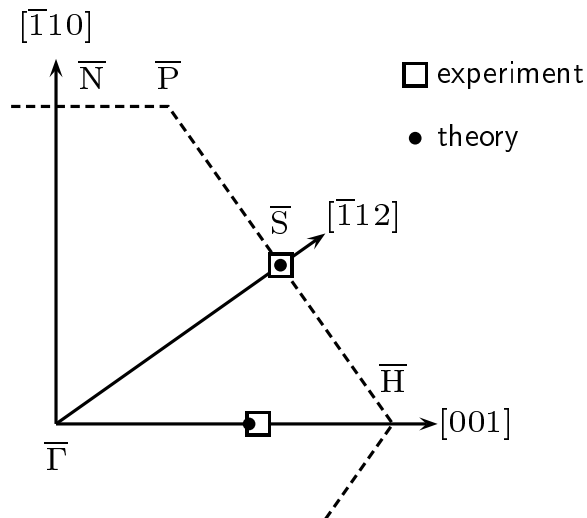


Fig. 4.  $\mathbf{k}$ -points loci of the HAS-measured (open squares) and calculated (full dots) critical wave vectors in the SBZ for H/Mo(110).

supported by a surface phonon, but the instability can not be removed via a Peierls distortion because of the large cost in elastic energy. Therefore, we expect low frequency oscillations of the electronic charge density near the Fermi level.

Because of these theoretical evidences we suggest the following interpretation of the experimental features. It is well known that for metal surfaces the turning point of the helium atoms in a HAS experiment is at a distance of about 3-4 Å in front of the surface and that the scattering potential depends on the electron density. The probe particles thus will sense electron charge density oscillations close to the Fermi level.<sup>33</sup> For the system Mo(110) at the critical wave vectors these oscillations are associated with electron-hole pair excitations involving the  $(d_{3z^2-r^2}, d_{xz})$  band. We therefore propose that the two bands seen by HAS are due to a hybridization between lattice vibrations and electron-hole pairs. Thus these studies represent an experimental manifestation of a nearly one-dimensional Kohn anomaly. While the small dip has a stronger phonon like character, the sharp and giant anomaly is due to a more electron-

hole like excitation. Balden<sup>34</sup> has recently found that the small indentation has indeed a temperature dependence like that of a phonon: Its frequency increases with increasing temperature. Furthermore, it has been observed<sup>2,3</sup> that the anomalies persist in the phonon dispersion curves along directions deviating from  $\overline{\Gamma\text{H}}$ , which is well understandable in terms of the theoretical results of Fig. 2c, because nesting is present also for the directions in the surface Brillouin zone out of the [001] azimuth. Because of the form of the  $(d_{3z^2-r^2}, d_{xz})$  band Fermi-surface contour, the anomalies should be particularly strong along  $\overline{\Gamma\text{S}}$  in agreement with the available experimental data.<sup>3</sup> In Fig. 4 we show the comparison between the experimental points in the SBZ, where the anomalies have been measured, and the points, where large section of the calculated Fermi surface contours are nearly parallel. The agreement is very good. We expect a weakening of the indentations for directions between  $\overline{\Gamma\text{H}}$  and  $\overline{\Gamma\text{S}}$  because of the less effective nesting. Unfortunately, no dispersion curves for the other two wave vectors mentioned in the literature<sup>2,3</sup> are available. A careful reanalysis of the experimental data is in progress.<sup>32</sup>

Our interpretation of the HAS results also explains why in HREELS only the Rayleigh mode with the small dip can be detected. In the impact regime electrons are scattered mainly by the ion cores and map the phonon dispersion curves. However, they are practically insensitive to electronic charge density oscillations.<sup>33</sup> Because the sharp and giant anomaly has only little vibrational character, it is practically impossible to excite it by high-energy electrons.

An open question is why the ARP measurements for the hydrogen covered Mo(110) and the theoretical Kohn-Sham Fermi surface are so much different. The results of Fig. 2c are due to photoelectrons which carry the information about the difference of the  $N$  particle ground state and the  $N - 1$  particle system with a hole at  $|\epsilon_F, \mathbf{k}\rangle$ . Typically an analysis surmises that the electronic system is in its ground state and that vibrational excitations as well as interactions between electronic and vibrational excitations can be neglected. The theoretical results shown in Fig. 2c, which are obtained under exactly this hypothesis, disclose that for this system the assumption may not be valid. In fact, the calculations predict highly localized parallel bands at the Fermi surface with a one-dimensional nesting vector. As a consequence, at  $\mathbf{Q}_{c1}$  and  $\mathbf{Q}_{c2}$  many electron-hole pairs will be thermally excited, and these will couple to phonons. This produces a breakdown of the Born-Oppenheimer approximation. While the calculations identify a strong nesting, the ARP experiments investigate a system which has already reacted to this nesting instability. When a static distortion is frustrated, ARP will measure a state with a significant number of low energy excitations (see Fig. 3), and in particular at the critical

wave vectors the electron and lattice dynamics cannot be decoupled. In fact, we note that the experimental Fermi surface of the H covered surface seems to display a lack of the translational symmetry associated with the  $(1 \times 1)$  SBZ (see the band circuits at the  $\bar{S}$  point in Fig. 2d). We cannot rule out, however, that this is due to inaccuracies in the experimental data or analysis. We are not aware that for any other surface such a serious breakdown of the Born-Oppenheimer approximation (compare Figs. 2c and d) has been observed so far. Obviously, the static distortion of the W(100) surface is also induced by a Kohn anomaly, but after the reconstruction has taken place the Born-Oppenheimer approximation is valid again. Some doubts remain at this point if an alternative explanation exists reconciling the differences of the experimental ARP data and the calculated results.

It is interesting to note that the energy barrier between two hollow sites is about 0.2 - 0.3 eV. This is, however, a rough estimate, because the results of Table 1 do not correspond to a single H-atom hopping event but to a displacement of the whole H layer. Nevertheless, it is in fact likely that at room temperature the full hydrogen monolayer might be dynamically strongly disordered: At a snapshot picture some H atoms may occupy the tip down triangles and others the tip up triangles. In this way a liquid like behaviour may result. We note, however, that because of the lack of isotopic effects in the characteristics of the phonon branch indentations, we discard any direct involvement of hydrogen vibrations in the anomaly mechanism.

### 3. Conclusion

In conclusion, the calculated Kohn-Sham Fermi surface can explain the HAS and HREELS experiments. It is interesting that the same band which is responsible for the pronounced anomaly identified above for Mo(110) produces in fact notable features of all group VIA materials. In particular we mention the spin-density wave in bulk Cr and the phonon anomalies along the [001] direction in bulk W and Mo. Also the reconstruction of Mo(100) and W(100) is induced by the nesting of this band. What makes the anomaly at the (110) so particularly strong is that the adsorption of hydrogen shifts it into a region of  $\mathbf{k}$ -space where it becomes localized at the surface. Thus the band becomes two- and the nesting one-dimensional. Neither the hydrogen wave functions nor the hydrogen vibration are *directly* involved in the resulting anomalies. The effect of hydrogen is mainly to change the potential at the surface and to shift the Mo surface states. Thus, it is well possible, that other adsorbates can influence in a similar way the surface vibrations and electron-phonon coupling. We also expect that for the clean surface a weak signature of the  $(d_{3z^2-r^2}, d_{xz})$

band should exist at  $Q \approx 0.6 \text{ \AA}^{-1}$ . However, for the clean surface the band is not a surface state but a broad and less localized surface resonance. The thermal excitations of electron-hole pairs at H/Mo(110) and the suggested breakdown of the Born-Oppenheimer approximation call for additional photoemission experiments, in which the Fermi surface is carefully studied also at lower temperatures. Furthermore, calculations of the electron-phonon coupling, electron-hole excitations and frozen phonons at these surfaces would be very helpful.

#### 4. Acknowledgments

We thank M. Balden, J. Lüdecke, E. Hulpke, and E. Tosatti for stimulating discussions.

#### References

1. E. Hulpke and J. Lüdecke, Surf. Sci. **272**, 289 (1992); Phys. Rev. Lett. **68**, 2846 (1992).
2. E. Hulpke and J. Lüdecke, Surf. Sci. **287/288**, 837 (1993); J. Electron. Spectr. Relat. Phenom. **64/65**, 641 (1993).
3. J. Lüdecke, Ph.D. thesis, Universität Göttingen(1994).
4. J. W. Chung, S. C. Ying, P. J. Estrup, Phys. Rev. Lett. **56**, 749 (1986).
5. M. Altman, J. W. Chung, P. J. Estrup, J. M. Kosterlitz, J. Prybyla, D. Sahu, and S. C. Ying, J. Vac. Sci. Technol. **A** 5, 1045 (1987).
6. B. Renker, L. Pintschovius, W. Gläser, H. Rietschel, and R. Comes, in *Lecture Notes in Physics*, Vol. 34 (Springer, Berlin, 1975), p. 53.
7. H.-J. Ernst, E. Hulpke, and J. P. Toennies, Phys. Rev. Lett. **58**, 1941 (1987); Europhys. Lett. **10**, 747 (1989); Phys. Rev. B **46**, 16081 (1992).
8. E. K. Schweizer and C. T. Rettner, J. Vac. Sci. Technol. A **7**, 1937 (1989).
9. E. Hulpke and D.-M. Smilgies, Phys. Rev. B **40**, 1338 (1989).
10. K. E. Smith, G. S. Elliott, and S. D. Kevan, Phys. Rev. B **42**, 5385 (1990).
11. J. W. Chung *et al.*, Phys. Rev. Lett. **69**, 2228 (1992).
12. L. Jupille and D. A. King, in *The Chemical Physics of Solid Surfaces, Vol. 7*, ed. by D. A. King and D. P. Woodruff (Elsevier, Amsterdam, 1994), p. 35.
13. K. H. Jeong, R. H. Gaylord, and S. D. Kevan, Phys. Rev. B **38**, 10302 (1988).
14. K. H. Jeong, R. H. Gaylord, and S. D. Kevan, Phys. Rev. B **39**, 2973 (1989); J. Vac. Sci. Technol. A **7**(3), 2199 (1989).
15. R. H. Gaylord, K. H. Jeong, and S. D. Kevan, Phys. Rev. Lett. **62**, 2036 (1989).

16. M. Balden, S. Lehwald, E. Preuss, and H. Ibach, *Surf. Sci.* **307/309**, 1141 (1994).
17. M. Balden, S. Lehwald, H. Ibach, and D. L. Mills, *Phys. Rev. Lett.* **73**, 854 (1994).
18. R. P. Feynman, *Phys. Rev.* **94**, 262 (1954).
19. B. Kohler, P. Ruggerone, S. Wilke, and M. Scheffler, *Phys. Rev. Lett.* **74**, 1387 (1995).
20. D. M. Ceperley and B. J. Alder, *Phys. Rev. Lett.* **45**, 566 (1980); J. P. Perdew and A. Zunger, *Phys. Rev. B* **23**, 5048 (1981).
21. P. Blaha, K. Schwarz, P. Sorantin, and S. B. Trickey, *Comput. Phys. Commun.* **59**, 399 (1990); P. Blaha, K. Schwarz, R. Augustyn, WIEN93, Technische Universität Wien, 1993.
22. R. Yu, D. Singh, and H. Krakauer, *Phys. Rev. B* **43**, 6411 (1991).
23. B. Kohler, S. Wilke, and M. Scheffler, to be published.
24. K. W. Katahara, M. H. Manghnani, and E. S. Fisher, *J. Phys. F* **9**, 773 (1979).
25. M. Methfessel, D. Hennig, and M. Scheffler, *Phys. Rev. B* **46**, 4816 (1992).
26. M. Methfessel, C. O. Rodriguez, and O. K. Andersen, *Phys. Rev. B* **40** (1989) 2009.
27. S. Wilke, D. Hennig, and R. Löber, *Phys. Rev. B* **50**, 2548 (1994).
28. P. J. Feibelman, *Phys. Rev. B* **43**, 9452 (1991); *Phys. Rev. Lett.* **67**, 461 (1991).
29. D. A. Papaconstantopoulos, *Handbook of the Band Structure of Elemental Solids* (Plenum, New York, 1986).
30. R. Hoffmann, *Rev. Mod. Phys.* **60**, 601 (1988).
31. E. Tosatti, *Festkörperprobleme* **15**, 113 (1975).
32. E. Hulpke, private communication.
33. C. Kaden, P. Ruggerone, J. P. Toennies, G. Zhang, and G. Benedek, *Phys. Rev. B* **46**, 13509 (1992); G. Benedek, J. Ellis, N. S. Luo, A. Reichmuth, P. Ruggerone, and J. P. Toennies, *Phys. Rev. B* **48**, 4917 (1993).
34. M. Balden, private communication.